

RESEARCH

Open Access



Hydrogen gas inhalation ameliorates LPS-induced BPD by inhibiting inflammation via regulating the TLR4–NFκB–IL6/NLRP3 signaling pathway in the placenta

Yafang Zhang¹, Xianhui Ren², Linli Zhang¹, Xinliu Sun³, Wenjing Li⁴, Yunxi Chen⁵, Yan Tian⁵, Zhongxia Chu¹, Youzhen Wei³, Guo Yao^{1*†} and Yan Wang^{1*†}

Abstract

Introduction Hydrogen (H₂) is regarded as a novel therapeutic agent against several diseases owing to its inherent biosafety. Bronchopulmonary dysplasia (BPD) has been widely considered among adverse pregnancy outcomes, without effective treatment. Placenta plays a role in defense, synthesis, and immunity, which provides a new perspective for the treatment of BPD. This study aimed to investigate if H₂ reduced the placental inflammation to protect the neonatal rat against BPD damage and potential mechanisms.

Methods We induced neonatal BPD model by injecting lipopolysaccharide (LPS, 1 μg) into the amniotic fluid at embryonic day 16.5 as LPS group. LPS + H₂ group inhaled 42% H₂ gas (4 h/day) until the samples were collected. We primarily analyzed the neonatal outcomes and then compared inflammatory levels from the control group (CON), LPS group and LPS + H₂ group. HE staining was performed to evaluate inflammatory levels. RNA sequencing revealed dominant differentially expressed genes. Bioinformatics analysis (GO and KEGG) of RNA-seq was applied to mine the signaling pathways involved in protective effect of H₂ on the development of LPS-induced BPD. We further used qRT-PCR, Western blot and ELISA methods to verify differential expression of mRNA and proteins. Moreover, we verified the correlation between the upstream signaling pathways and the downstream targets in LPS-induced BPD model.

Results Upon administration of H₂, the inflammatory infiltration degree of the LPS-induced placenta was reduced, and infiltration significantly narrowed. Hydrogen normalized LPS-induced perturbed lung development and reduced the death ratio of the fetus and neonate. RNA-seq results revealed the importance of inflammatory response biological processes and Toll-like receptor signaling pathway in protective effect of hydrogen on BPD. The over-activated upstream signals [Toll-like receptor 4 (TLR4), nuclear factor kappa-B p65 (NF-κB p65), Caspase1 (Casp1) and NLR family pyrin domain containing 3 (NLRP3) inflammasome] in LPS placenta were attenuated by H₂ inhalation. The downstream targets, inflammatory cytokines/chemokines [interleukin (IL)-6, IL-18, IL-1β, C–C motif chemokine

[†]Guo Yao and Yan Wang contributed equally to this work.

*Correspondence:

Guo Yao

tayg8005@126.com

Yan Wang

vicky2000love@163.com

Full list of author information is available at the end of the article



ligand 2 (CCL2) and C-X-C motif chemokine ligand 1 (CXCL1)], were decreased both in mRNA and protein levels by H₂ inhalation in LPS-induced placentas to rescue them from BPD. Correlation analysis displayed a positive association of TLR4-mediated signaling pathway both proinflammatory cytokines and chemokines in placenta.

Conclusion H₂ inhalation ameliorates LPS-induced BPD by inhibiting excessive inflammatory cytokines and chemokines via the TLR4–NFκB–IL6/NLRP3 signaling pathway in placenta and may be a potential therapeutic strategy for BPD.

Keywords Hydrogen, BPD, Placenta, Inflammation, TLR4, NFκB, NLRP3

Introduction

Owing to the lack of effective interventions to prevent preterm births and life-saving postpartum intervention, BPD has been recognized as the most frequent complication in premature infants and is accompanied by high incidence and poor prognosis [1]. It can lead to the development of chronic lung dysfunction and persistent airway and pulmonary vascular diseases, seriously affecting survival quality [2, 3].

BPD is now considered the result of an abnormal repair response to lung injury by multiple antenatal and postnatal exposures [4]. The etiology and pathogenesis of BPD are complex. (1) It is well known that inflammation is the key to the occurrence of BPD, whether prenatal or postpartum. Especially, chorioamnionitis (CAM) is expressed as the common antenatal pathway that initiates lung injury that can progress to a BPD phenotype [5]. CAM is an independent risk factor for the occurrence of BPD, as well as the most common and important factor in clinic. When the pathogen infects the amniotic cavity through ascending transmission, causing chorioamnionitis, the placenta releases a large number of inflammatory factors into the fetal blood circulation, resulting in the accumulation of inflammatory factors in the fetal lung, which lead to the decrease of the expression of lung cytokines, turn out fetal pulmonary developmental disorders. In addition, the release of placental chemokines promotes the infiltration of proinflammatory cells in fetal lung tissue, affects the development of alveoli and eventually leads to the occurrence of BPD. (2) Postpartum infection: mainly found in preterm infants with severe pneumonia, NEC, sepsis, etc. Due to immunodeficiency in preterm infants, systemic inflammatory response syndrome develops rapidly when combined with severe infection. Substantial numbers of inflammatory factors are released into the blood circulation and aggregated in the pulmonary circulation, which also leads to lack of ventilation and hypoxia to further aggravate the lung injury, resulting in the occurrence of BPD. (3) Hyperoxia: mainly occurs in long-term oxygen dependence of premature infants. Lack of relatively mature antioxidant capacity in premature infants, oxygen free radicals increase significantly

when exposed to hyperoxia. Abundant oxygen free radicals accumulate in the lung, which further initiate inflammation, apoptosis and other signal pathways, resulting in lung injury and promoting the occurrence of BPD. (4) Ventilator application: due to the immature lung development of premature infants, ventilator is required to provide high airway pressure and high tidal volume to maintain normal breathing and blood oxygen saturation to rescue. Unfortunately, airway pressure damage is also accompanied by, which can induce the lung infection and oxidative stress, in turn, give rise to the obstruction of pulmonary development. (5) In addition, preeclampsia, vitamin deficiency, smoke exposure and genetic susceptibility are also high risk factors for BPD. Although the pathogenesis of BPD is complex, inflammation plays a primary role in the BPD onset. Inhibition of inflammatory responses is particularly crucial to reduce BPD.

Placenta, as a bridge between maternal to fetus and owing to the advantage of the available clinical specimens, has gradually become a hot topic for the study of perinatal neonatal diseases. With the continuous excavation of placental function, placenta not only acts as a key medium for maternal–infant nutrition exchange, but also as the regulatory hub located between the maternal and the fetus, which plays a role in the regulation of inflammation, gradually arouse widespread concern and become the focus of research. Placental components, such as proinflammatory factors and chemokines, can promote the activation of inflammatory cells such as monocytes and macrophages. On the other hand, it can enhance the migration of proinflammatory cells. Increasing evidence linking the inflammatory regulatory function in the placenta to BPD has been analyzed in a systematic review [6]. The placenta makes an adaptive response to CAM induced by LPS [7], and even placental histology is believed to predict adverse neonatal outcomes in some studies, which can cause the aggregation of placental decidual cells, amniotic cells and infiltrating macrophages and release proinflammatory cytokines and chemokines to the gestational sac [8], subsequently resulting in fetal inflammatory response syndrome (FIRS) and eventually contributing to the

development of BPD [9, 10]. Concerning the vital role of the placenta in anti-inflammation, it is conceivable that alterations of the placenta can reverse the process of LPS-induced BPD and result in improving the poor prognosis that has lifelong consequences.

Hydrogen, a novel therapeutic molecule, mainly exerts anti-inflammatory, antioxidant and anti-apoptosis effects, which have been confirmed by many cellular, animal and clinical trials [11–13]. Despite many inaccuracies, inflammation scavenging ability is still the widely accepted mechanism of H₂ [14, 15]. Lack of any known adverse effects of hydrogen makes hydrogen an ideal anti-inflammatory therapeutic modality [16, 17].

Therefore, the purpose of this study was to investigate the protective effect of hydrogen in placenta against LPS-induced BPD and to explore its underlying molecular mechanisms.

Methods

A neonatal rat model of BPD and experimental design

All experimental procedures were approved by the Medical Ethics Committee of the affiliated Taian City Central Hospital of Qingdao University in Shandong, China (permit numbers: 2022-07-10). Eight-week-old Sprague–Dawley (SD) rats were purchased from Shanghai JSJ. Male and female rats with a ratio of 1:2 were caged overnight, and vaginal plugs were confirmed the next morning, which was counted as E0.5. We induced CAM to generate a neonatal rat model of BPD by injecting LPS (0.2 µg/µl, 5 µl) into the amniotic fluid at E16.5. LPS from *Escherichia coli* (O55:B5) was purchased from Sigma–Aldrich (L2880, Shanghai, CHINA).

Administration of hydrogen gas

To study the protective effect of hydrogen inhalation in the neonatal model of BPD, pregnant rats were randomly divided into three groups: a normal control group (CON group, *n* = 5), a LPS-induced BPD group (LPS group, *n* = 5), and a hydrogen administration group (LPS + H₂ group, *n* = 5). The numbers of gestational sacs were 50 in CON group, 46 in the LPS group, and 48 in LPS + H₂ group. After the intra-amniotic injection of LPS, pregnant rats in LPS + H₂ group were immediately placed in a hydrogen treatment warehouse with 42% hydrogen and 21% oxygen for continuous hydrogen absorption (4 h/day) until the samples were collected. The body of the warehouse is transparent to ensure visibility.

Animal specimen collection

The placenta and umbilical cord were collected by cesarean section at E21.5, and the weights of the neonates and placentas were recorded. The newborn rats were fed breast-feeding rats prepared in advance. The intrauterine

fetal death (IUFD) rate was calculated by the number of stillbirths based on fetal counts at E16.5. The number of surviving pups was continuously counted until postnatal day (P) 14. The body weights of pups were measured at P0, P7 and P14.

The research processed the placental tissue and umbilical cord during cesarean section and collected the left lung of neonatal rats at P0, P7 and P14 for hematoxylin–eosin (HE) staining and further analysis to determine the contribution of inhaled hydrogen to BPD. Pups were euthanized at P7 and P14 by an intraperitoneal injection of 120 mg/kg (2 ml/kg) sodium pentobarbital, followed by cardiac perfusion with precooled saline. The placentas were placed in the tubes and stored frozen at –80 °C for RNA-seq, ELISA, qRT-PCR and Western blot assays.

Histological examinations

To intuitively evaluate the degree of LPS-induced CAM and assess the perturbed lung development, all specimens, including the placentae, umbilical cords and pup lungs, were fixed by mage-iT™ Fixative Solution (4% paraformaldehyde in PBS) (Thermo Fisher Scientific Inc, USA) according to protocol of hematoxylin–eosin (HE) Stain Kit (Solarbio Science & Technology Co., Beijing, CHINA). After washing, gradient alcohol for dehydration, transparent in xylene and subsequently paraffin-embedded and cut into 5-µm-thick sections. Dewaxing twice in xylene for 10 min, and series of alcohol (100%, 95%, 85%, 75%) for 3 min in turn to hydrate to water. Hematoxylin solution stained the nucleus for 10 min and rinsed in running tap water. Followed by differentiation and re-dyeing with Eosin solution for 30 s. Finally, samples were dehydrated, rendered transparent and sealed with neutral gum. Sections were observed under a microscope and photographed. Parameters of alveolarization: the mean linear intercept (MLI), radial alveolar count (RAC) and alveolar wall ratio (alveolar wall area/total area) were measured.

RNA sequencing (seq)

To reveal the molecular mechanism of specific biological processes and the protective effects of inhaled H₂ on the occurrence of LPS-induced BPD, RNA sequencing analysis of placental tissue was performed in the experiment. According to the manufacturer's protocol, the process was as follows: the total RNA was extracted by a TRIzol reagent kit (Invitrogen, Carlsbad, CA, USA), and enriched into mRNA after the quality assessment. The enriched mRNA was then fragmented into short fragments and reverse-transcribed into cDNA using the NEBNext Ultra RNA Library Prep Kit for Illumina (NEB#7530, New England Biolabs, Ipswich, MA, USA).

Subsequently, adding A base, ligating the cDNA to Illumina sequencing adapters. The target fragment was recovered by agarose gel electrophoresis and amplified by PCR, ultimately completing the preparation of the whole library, and the constructed library was sequenced using an Illumina Novaseq6000 by Gene Denovo Biotechnology Co. (Guangzhou, China).

Furthermore, performing the biological analysis process to identify metabolic signaling pathways involved. A FPKM (fragment per kilobase of transcript per million mapped reads) value was calculated to quantify the expression abundance and variations by RSEM software. To identify the differentially expressed genes, we performed the analysis by DESeq2 software between two different groups. Parameters of the genes/transcripts were considered differentially statistically significant when q -value < 0.05 (the corrected p -values obtained by the BH algorithm) and absolute fold change ≥ 2 . Differentially expressed genes were mapped to GO terms in the Gene Ontology database (<http://www.geneontology.org/>), gene numbers were calculated for every term, and significantly enriched GO terms in DEGs compared to the genome background were defined by a hypergeometric test. Kyoto Encyclopedia of Genes and Genomes (KEGG) pathway enrichment analysis was performed to identify significantly enriched metabolic pathways and signal transduction pathways in DEGs.

Quantitative real-time polymerase chain reaction (qRT-PCR) assay

The mRNA levels of dominant differentially expressed genes screened by RNA-seq were verified by qRT-PCR. Total RNA was extracted from 100 mg of placental tissue using the TRIzol method (Invitrogen, Life technologies, USA), and was reverse-transcribed to cDNA using HiFiScript gDNA Removal RT MasterMix (Cwbio Bio Inc., Beijing, CHINA). The qRT-PCR assay was performed with Roche LightCycler 480 II Real-Time PCR System with MagicSYBR Mixture (Cwbio Bio Inc., Beijing, CHINA). Each sample was configured to a 25- μ l reaction volume with β -actin as a reference gene. Reaction conditions were as follows: pre-denaturation at 95 °C for 10 min, followed by 45 cycles of denaturation at 95 °C for 5 s, annealing at 60 °C for 30 s. The melt curve was set with the parameters (95 °C for 15 s, 60 °C for 1 min, 95 °C for 15 s and 50 °C for 30 s). The design of experimental primers followed the basic principles of primer design: the primer length was 18–25 bp, and the gap between sense and anti-sense was less than 3 bp. The length of the amplified product should be controlled within 300 bp. Four bases should be randomly distributed to avoid base accumulation. Selecting the G and C bases at the 3' end of the primer avoid autohybridization

binding and dimerization. Melting temperature (T_m): sense and anti-sense should have similar T_m , with a difference of less than 5 °C. Research protocol: in the 'Nucleotide' section of NCBI, input the gene and species names, then download the nucleotide sequences, and use the BLAST tool on NCBI for sequence alignment. After obtaining the gene sequences, Primer Premier 5 software was used to design primers by analyzing dimers, false promoters, cross dimers, and hairpins to analyze their specificity. The sequence of primers, product length and optimal annealing temperature (T_a opt) are shown in Table 1.

Western blot

Western blot analysis was performed on placental tissues from CON, LPS, LPS + H₂ groups. The placental tissue was rinsed in precooled saline to remove blood and placed in an EP tube with a steel bead. 500 μ l lysate including phosphatase inhibitor cocktail, protease inhibitor cocktail and RIPA lysis buffer with 1:100 ratio were added to the EP tube to homogenize for 50 s at 40 HZ, then incubated for 30 min (–20 °C for 10 min and 4 °C for 20 min). The protein supernatant was extracted by centrifugation at 12,000 rpm 4 °C for 30 min. Adopting the BCA Protein Assay Kit (Thermo Fisher Scientific, MA, United States) to quantify the protein concentration and diluted by using the Omni-Easy™ Protein Sample Loading Buffer to guarantee all samples a final protein concentration of 2 μ g/ μ l based on the calculated protein concentration. The extracted total protein was denatured by boiling for 5 min at 100 °C after addition of protein 4 \times Buffer. The target proteins were isolated from 40 μ g (loading amount was 40 μ g with volume of 20 μ l) of protein samples using the Bio-Rad system (Bio-Rad, Shanghai, USA) with 10% PAGE Gel Fast Preparation Kit (Epizyme Biotech., Shanghai, CHINA) (the parameters of electrophoresis: voltage 80 V run to the end of the concentrated gel, and adjust to 160 V until the bottom of the glass plate in Tris/Glycine/SDS Running Buffer), and next, transferred to PVDF membranes using precooled transferring buffer (The transfer parameter was set as current 300 mA and transfer times were set according to the molecular weight of primary antibody with 1:1 ratio) and blocked in 5% skimmed milk for 3 h at least. The PVDF membranes were incubated overnight with different antibodies at 4 °C: Rabbit monoclonal to NLRP3 (Abcam, ab263899, USA, 1:1000), Rabbit polyclonal to TLR4 (Abcam, ab217274, USA, 1:1000), Rabbit monoclonal to NF- κ B p65 (phospho S536) (Abcam, ab76302, USA, 1:1000), Rabbit Anti-NF κ B p65 antibody (Bioss, bs-0465R, CHINA, 1:800), Anti-CASP1 Rabbit polyclonal antibody (Merck, SAB5701133, CHINA, 1:1000), I κ B α Rabbit pAb (ABclonal, A1187, CHINA,

Table 1 The sequence, product length and Ta opt of primers used for qRT-PCR analysis

Gene	Primer sequence 5' to 3'	Product length	Ta Opt
TLR4	Sense 5'-TGGTGGCTGTGGAGACAAAATGAC-3' Anti-sense 5'-CTGAAAGGCTTGGGCTTGAATGGAG-3'	281	53.1
Nfkb α /IkBa	Sense 5'-CTGTACGCCCCAGCATCT-3' Anti-sense 5'-GCACCCAAAGTCACCAAG-3'	123	53.2
NF-kBp65/Rela	Sense 5'-ATCCCTGCTTCCCTTTCTC-3' Anti-sense 5'-CTGTCTTATGGCTGAGGTCTGGT-3'	88	52.5
IL-6	Sense 5'-ATTGTATGAACAGCGATGATGCAC-3' Anti-sense 5'-CCAGGTAGAAACGGAACTCCAGA-3'	150	51.3
CXCL1	Sense 5'-ACTCCAGCCACACTCCAACA-3' Anti-sense 5'-GCGGCATCACCTTCAAATC-3'	190	57.3
CCL2	Sense 5'-GTGCTGACCCCAATAAGGAA-3' Anti-sense 5'-TGCTGAAGTCCTTAGGGTTGA-3'	116	49.9
NLRP3	Sense 5'-TGAAGAGTGTGATCTGCGGAAAC-3' Anti-sense 5'-GAAAGTCATGTGGCTGAAGCTGT-3'	124	53.5
Casp1	Sense 5'-CGGGCAAGCCAGATGTTTAT-3' Anti-sense 5'-AACCACTCGGTCCAGGAAATG-3'	193	52.5
IL-18	Sense 5'-GCAGTAATACGGAGCATAAA-3' Anti-sense 5'-ATCCTTCACAGATAGGGTCA-3'	177	50.3
IL-1 β	Sense 5'-TTCTTTGAGGCTGACGGACC-3' Anti-sense 5'-TGAGTCACAGAGGATGGGCT-3'	255	54.7
β -actin	Sense 5'-AGGGAAATCGTGCGTGACAT-3' Anti-sense 5'-GAACCGCTCATTGCCGATAG-3'	150	54.6

1:1000), Phospho-IkBa-S32 Rabbit mAb (ABclonal, AP0707, CHINA, 1:1000) and β -actin Rabbit Monoclonal Antibody (Beyotime, AF5003, CHINA, 1:2000) and incubated with HRP-labeled Goat Anti-Rabbit IgG (H+L) (Beyotime, A0208, CHINA, 1:1000) for 2.5 h at least at room temperature. β -actin was selected as the internal reference protein, which is not only a protein encoded by the housekeeper gene, but also highly conserved and expressed relatively stable. The expression of β -actin was not affected by hydrogen administration and inflammation. In addition, the molecular weight of β -actin was 42 kDa, suitable to distinguish the target protein.

Using the Omni-ECL™ Enhanced Pico Light Chemiluminescence Kit (Epizyme Biotech., Shanghai, CHINA) indicated the positive target strips. The relative protein expression used ALPHA Imager HP Gel imaging system and Image J software.

Cytokine and chemokine detection

To validate the levels of inflammatory response in the placenta, we used ELISA to measure proinflammatory cytokines and chemokines in placenta. Placental tissue was accurately weighed, rushed with balls at 4 °C, and stored overnight at -20 °C. After two freeze-thaw cycles, the supernatant was removed after the homogenates

were centrifuged at 5000 \times g for 5 min at 4 °C. The samples to be tested were separated and stored at -20 °C. The protein concentration was determined by a BCA protein assay kit (Thermo Fisher Scientific, MA, United States). Experimental protocols of different inflammatory factors were subject to the ELISA kit instructions. The kit had been coated in the reaction well and processed with antibodies. The steps were as followed: add sample: blank well, fold ratio diluted standard well, add 100 μ l of appropriately diluted sample to the reaction well and incubated at 37 °C for 1.5 h. Then washed to react to the diluted biotinylated antibody working solution at 37 °C for 1 h. Followed by reacting 30 min with 100 μ l of the working solution of the enzyme conjugate after washing. 100 μ l of TMB substrate solution was added to chromogenic reaction for 10–30 min, based on the obvious color gradient which appeared in the diluted standard well to terminate by adding 100 μ l of 2 M sulfuric acid. The OD value of each reaction well was measured on the enzyme meter, the standard curve was drawn, and then the sample concentration was calculated according to the standard curve equation. The contents of IL-6, CCL2, CXCL1, IL-1 β and IL-18 in placental tissues were determined by ELISA kits, including IL-6 uncoated ELISA Kit (Cat. no. 88-50625, Thermo Fisher Scientific, MA, United States), CCL2 ELISA Kit (Cat. no. EK387-96,

MULTI Scientific, Hangzhou, China), CXCL1 ELISA Kit (Cat. no. EK396, MULTI Scientific, Hangzhou, China), IL-1 β ELISA Kit (Cat. SEA563Ra, USCN KIT INC. Wuhan, China) and IL-18 ELISA Kit (Cat. SEA064Ra, USCN KIT INC. Wuhan, China).

Statistical analysis

Statistical analysis was performed with the GraphPad Prism 8.0 database. All results are presented as mean \pm SD, and $p < 0.05$ was considered significant. All data were analyzed using one-way analysis of variance (ANOVA) with Dunnett, except that GO and KEGG enrichment analyses in RNA-seq were performed using hypergeometric test and BH algorithm. Pearson correlation analysis was used to measure the relationship between NBW and placental weight and the relationship between the levels of TLR4–NF κ B–IL6/NLRP3 proteins and inflammatory factors.

Table 2 Maternal baseline characteristics in different groups

	CON	LPS	LPS + H ₂
Maternal rat (n)	5	5	5
Maternal weight (g)	298.80 \pm 7.83	301.00 \pm 8.25	285.60 \pm 5.44
Gestational sacs (n)	50	46	48
Fetal death (n)	3	18	13
IUFD rate (%)	6	39	27

Results

H₂ attenuated the abnormal intrauterine development induced by LPS

The neonatal outcome results were checked immediately after birth and are displayed in Table 2. Among the maternal baseline characteristics, the intrauterine fetal death (IUFD) rates were 3/50 (6%) in the CON group, 18/46 (39%) in the LPS group, and 13/48 (27%) in the LPS + H₂ group. Moreover, there was no significant difference in maternal weight or the number of amniotic sacs.

H₂ inhalation improved the poor outcomes of neonatal rats

Similarly, the pups in the LPS group represented a growth-restricted state in the postnatal days in Fig. 1, mainly in the lower body weight at P0–P14 (Fig. 1A) and lower survival rate up to P14 (Fig. 1B). However, dysplasia and the lower survival ratio were all improved by hydrogen in the LPS + H₂ group ($p < 0.01$).

Positive correlation between placental weight and BW

Compared with that in the CON group, the BW in the LPS group was significantly lower, as shown in Fig. 2A. Similarly, the average placental weight in the LPS group was also at a lower level, as shown in Fig. 2B. Interestingly, the above abnormalities were improved after hydrogen inhalation ($p < 0.05$). A positive relationship between placental weight and BW was found in pups at P0 ($r = 0.7528$; $p < 0.0001$; Fig. 2C).

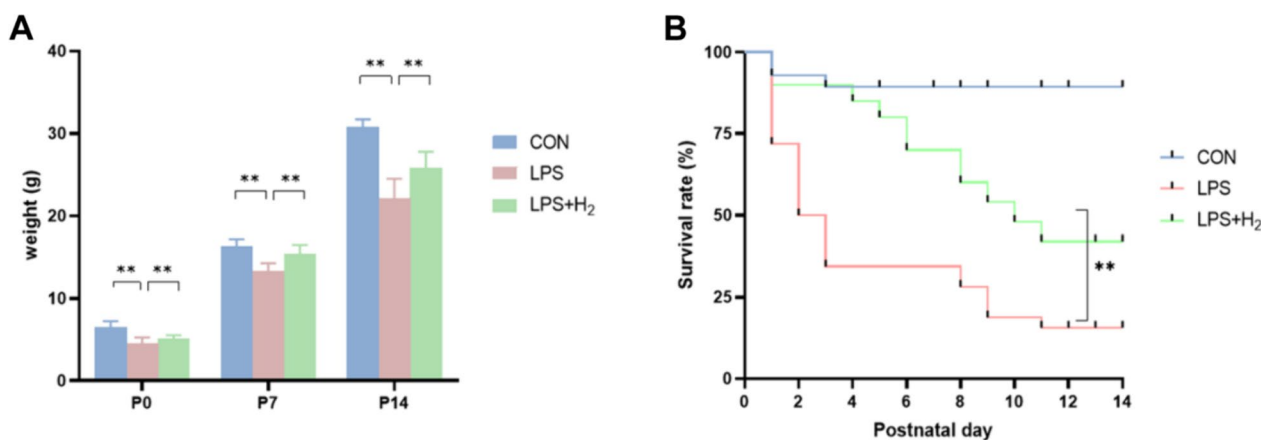


Fig. 1 The outcomes of neonatal rats dynamically from P0 to P14. **A** Body weights of pups at P0 (n = 15 for CON, 15 for LPS, and 15 for LPS + H₂) and P7 (n = 15 for CON, 12 for LPS, and 15 for LPS + H₂) and P14 (n = 12 for CON, 9 for LPS, and 12 for LPS + H₂). Data are presented as the mean \pm SD using ANOVA followed by Tukey’s multiple comparison test. * $p < 0.05$, ** $p < 0.01$ vs LPS group. **B** Kaplan–Meier survival curves of pups from P0 to P14 (n = 47 for CON, 28 for LPS and 35 for LPS + H₂). A significant difference was observed by the log-rank test ($p = 0.0017$)

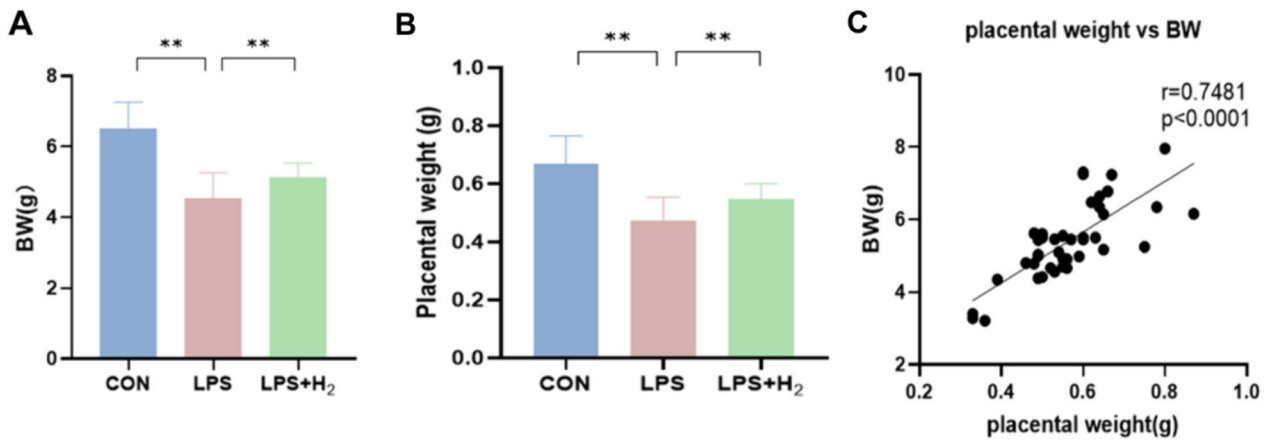


Fig. 2 The neonatal baseline characteristics in the CON, LPS and LPS +H₂ groups. **A, B** Birth weight (BW) and placental weight of pups (a total of 15 newborn rats were selected from each group (3 newborns were randomly selected from each maternal rat); n=15 for CON, 15 for LPS and 15 for LPS +H₂). *p<0.05, **p<0.01 vs LPS group. **C** Relationship between BW and placental weight in all groups (n=45), r= Pearson's correlation coefficient

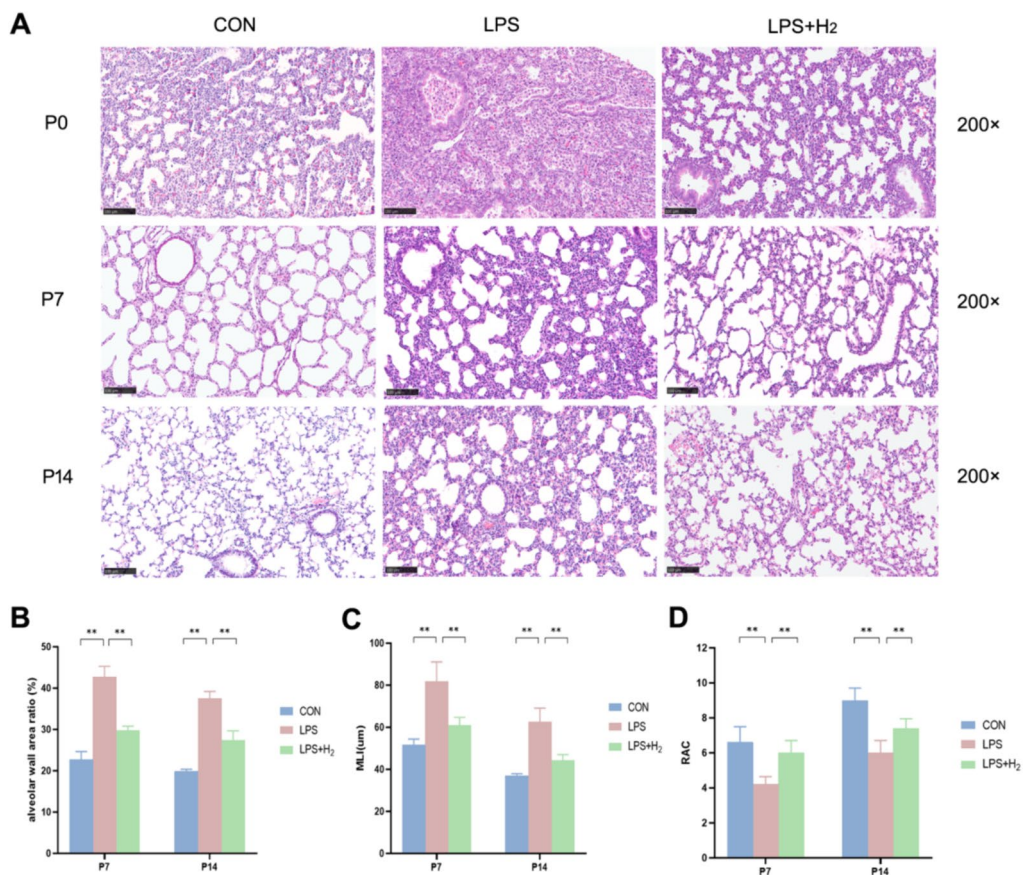


Fig. 3 Lung pathological histology in the CON, LPS and LPS +H₂ groups. **A** HE staining of lung tissues at P0, P7 and P14 (scale bar, 100 μm). **B** The alveolar wall area ratio: Image J software was used to quantitatively calculate the alveolar wall area and total area, and then the ratio was calculated to analyze the significant difference in the three groups (n=5). **C, D** Graphic representation of the abundance of the average mean linear intercept (ML) and radial alveolar count (RAC) at P7 and P14 in the three groups (n=5). *p<0.05, **p<0.01 vs LPS group

H₂ inhalation significantly relieved LPS-induced perturbed lung development

Perturbed lung development with an obvious lag was demonstrated in the LPS group by histological examination. LPS treatment abnormally increased the alveolar size, resulting in a heterogeneous alveolar and severe inflammatory response with a large amount of polymorphonuclear leukocyte infiltration. Fortunately, hydrogen normalized the alveolar sizes and pulmonary septum and evidently reduced inflammatory cell infiltration (Fig. 3A). Quantitatively, the parameters of alveolarization, the alveolar wall area ratio and the MLI, were increased by LPS, and the RAC was decreased by LPS. In contrast, the above disorder induced by LPS was normalized by hydrogen (Fig. 3B–D).

Hydrogen inhalation inhibited the excessive inflammatory response of LPS-induced placenta and fetus

Placentae in the LPS group displayed severe CAM, which manifested as a large amount of polymorphonuclear leukocyte infiltration (200×, Fig. 4), involving the lower pole of the amniotic sac, the intervillous space, the chorionic plate, decidua and even the whole layer of the placenta. Interestingly, upon administration of H₂, the infiltration degree was remarkably reduced, and the infiltration range significantly narrowed; only

the amniotic sac and chorionic plate were involved. Similarly, this phenomenon was also presented in the HE staining of umbilical cord, which reflected the degree of inflammation in the fetus. Unlike the CON group, inflammatory cells were scattered in the umbilical artery (200×, Fig. 5) and surrounding amniotic membrane (100×, Fig. 5) in the LPS group but not in the LPS+H₂ group.

The TLR4–NFκB–IL6/NLRP3 signaling pathway was involved in hydrogen inhalation rescue from LPS-induced inflammatory imbalance in the placenta

To further verify the underlying mechanisms of the H₂ effect, the transcriptome in the CON, LPS and LPS+H₂ groups was determined via RNA-seq. The RNA-seq data have been deposited in the NCBI Sequence Read Archive (SRA) database, with accession number PRJNA901070. Differentially expressed genes indicated that H₂ could have a therapeutic effect on LPS-induced BPD via various molecular mechanisms. A total of 671 genes with significant differences were screened out

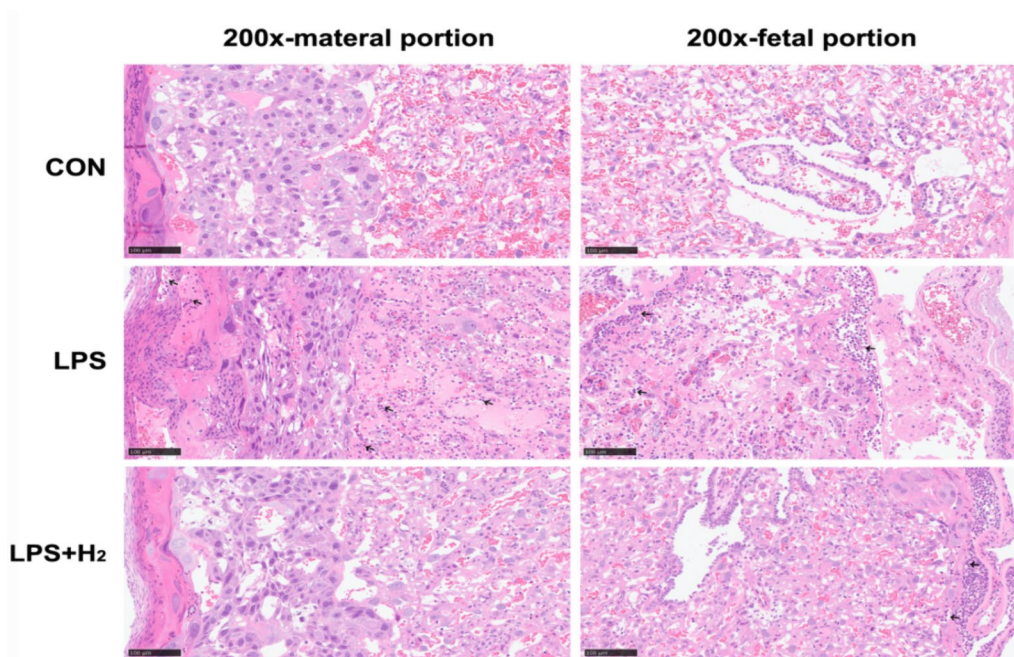


Fig. 4 Placental histologies by HE staining in the CON, LPS and LPS+H₂ groups. The 200× images show the maternal portion and fetal portion to present the degree of polymorphonuclear leukocyte infiltration. Black arrows indicated polymorphonuclear leukocyte infiltration in different portion of placenta

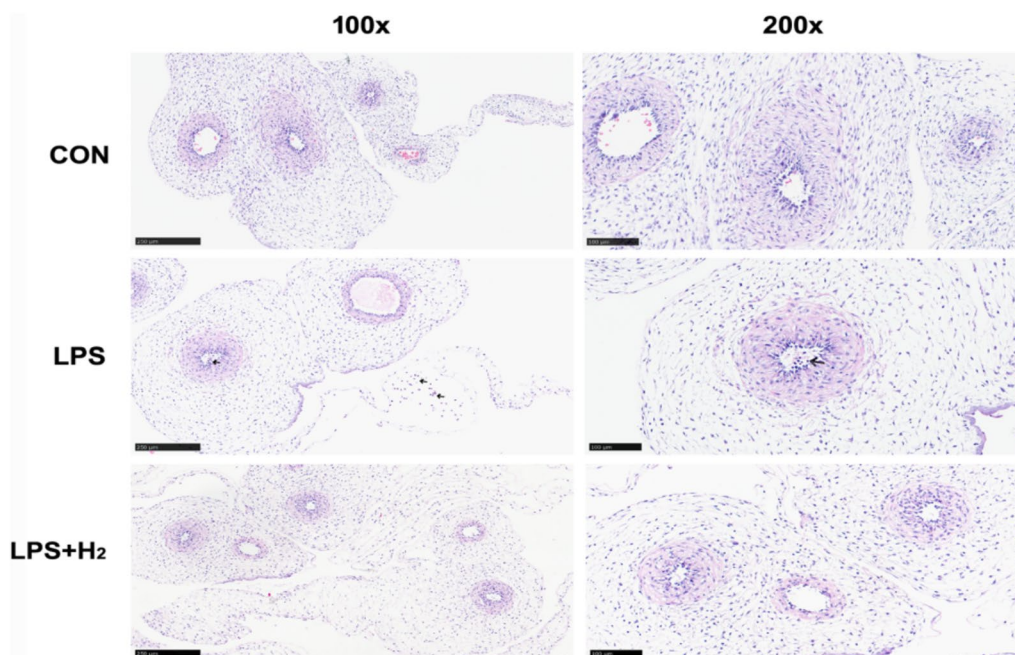


Fig. 5 Umbilical cord histologies by HE staining in the CON, LPS and LPS + H₂ groups. Inflammatory cells were pointed out with black arrows

when comparing the LPS + H₂ group with the LPS group, including 78 upregulated and 593 downregulated genes (Fig. 6A). Significantly enriched GO terms circular bar plot identified the outstanding ‘inflammatory response (GO:0006954)’ biological processes in placenta (Fig. 6B). To further elucidate the mechanism, KEGG pathway analysis was also applied to analyze the dysregulated genes involved in various signal transduction pathways. Among the top 20 KEGG enrichments, the Toll-like receptor signaling pathway was strikingly located (Fig. 6C).

Meanwhile, we screened multiple differentially expressed genes based on TLR-mediated inflammatory signaling pathway, and presented them as the FPKM levels (Fig. 6D). The increased mRNA levels of TLR4, NF- κ B inhibitor α (I κ B α), NLRP3 and Casp1 in LPS placenta were attenuated by H₂ inhalation. The downstream targets, overactive inflammatory cytokines/chemokines (IL-6, IL-18, IL-1 β , CCL2 and CXCL1) were also decreased in LPS + H₂ group.

H₂ inhalation inhibited inflammatory response via TLR4–NF κ B–IL6/NLRP3 inflammatory signaling pathway in placenta

Alterations of mRNA levels of TLR4–NF κ B–IL6/NLRP3 inflammatory signaling pathway in placenta

The RNA-seq results in this research revealed that the TLR4–NF κ B–IL6/NLRP3 signaling pathway was involved in the inflammatory response. Therefore, it was

hypothesized that H₂ may function via the TLR4–NF κ B–IL6/NLRP3 inflammatory signaling pathway. So, the study expanded the number of samples, and validated the mRNA expression by qRT-PCR analysis.

As shown in Fig. 7, placenta in LPS group had significantly higher mRNA levels of TLR4, I κ B α , NF- κ B p65(RelA), NLRP3, Casp1, IL-6, CXCL1, CCL2, IL-18 and IL-1 β ($p < 0.05$; Fig. 7A–J) compared to CON group. While, which were inhibited after inhaled hydrogen except for RelA ($p < 0.05$; Fig. 7A–J).

H₂ inhalation moderated the increased protein levels of the TLR4–NF κ B–IL6/NLRP3 signaling pathway and scavenged excessive placental inflammatory cytokines and chemokines

Compared to the CON group, the placental protein level of TLR4, p-I κ B α (s32), p-I κ B α (s32)/I κ B α , p-p65(s536), p-p65/NF- κ Bp65, NLRP3 and Casp1 in the LPS group was remarkably increased in response to LPS ($p < 0.05$; Fig. 8). Fortunately, inhaled H₂ moderated the above disorder ($p < 0.05$; Fig. 8). In addition, there was no significant difference in total NF- κ Bp65 and I κ B α protein levels between the three groups ($p > 0.05$; Fig. 8C and F).

The placenta in the LPS group exhibited an inflammatory storm. For instance, inflammatory cytokines such as IL-6, IL-18, IL-1 β and inflammatory chemokines such as CCL2 and CXCL1 were excessively released by placental cells ($p < 0.05$; Fig. 9A–E). When H₂

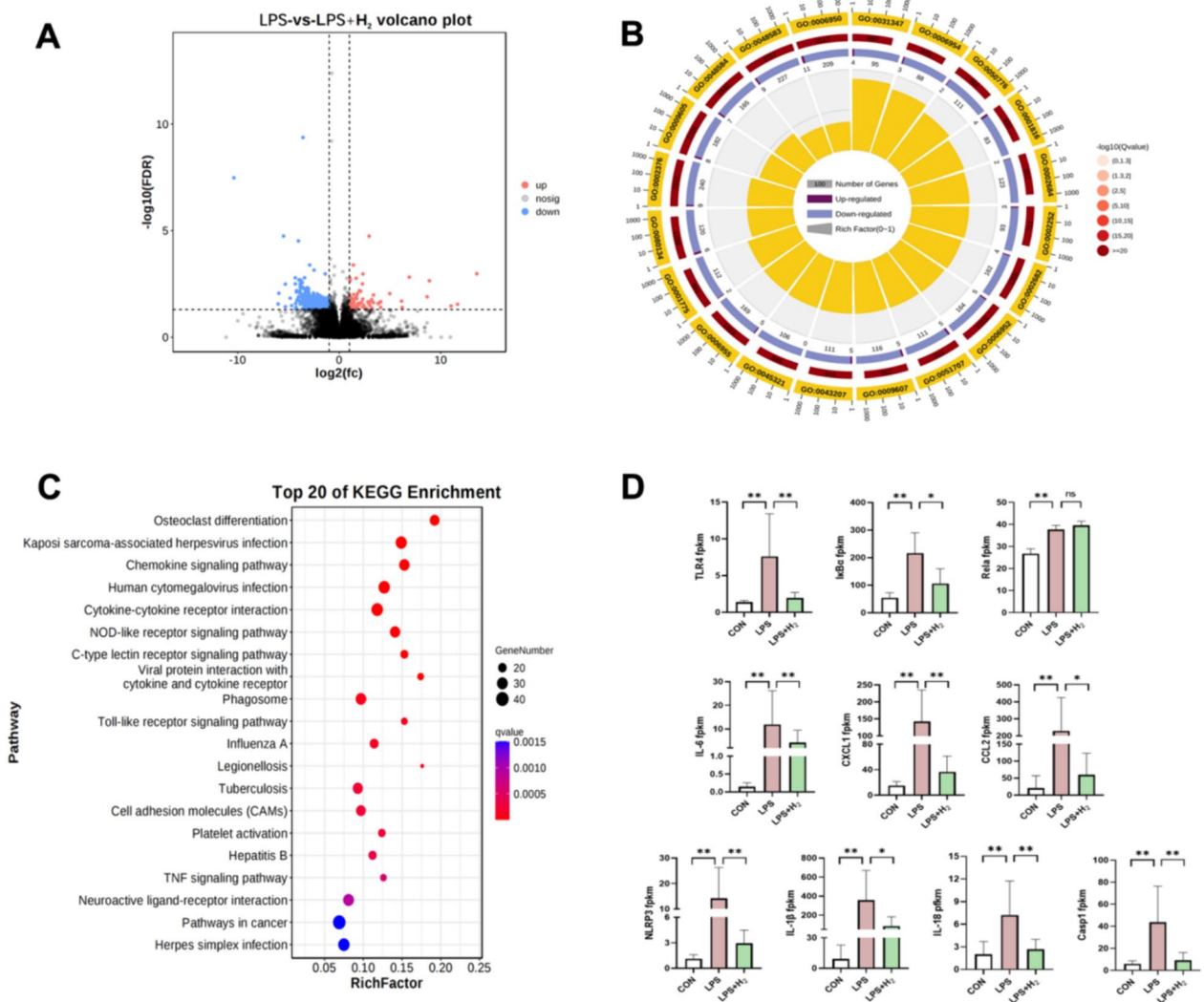


Fig. 6 Hydrogen reversed the dysregulated placental genes of the TLR4–NFκB–IL6/NLRP3 inflammatory signaling pathway in response to LPS. **A** Placentae in the LPS group and LPS + H₂ group were sent for RNA-seq. A volcano plot map of the differentially expressed genes was identified with cut-off values of q -value < 0.05 and $|\log_2(\text{fc})| > 1$, in which red represented upregulated genes and blue represented downregulated genes. **B**, **C** GO and KEGG enrichment analyses were performed with the differentially expressed genes. **D** The FPKM levels of the TLR4–NFκB–IL6/NLRP3 signaling pathway ($n = 4$). * $p < 0.05$, ** $p < 0.01$ vs LPS group, q -value: the corrected p -values obtained by the BH algorithm were conceptually equivalent to adjusted p -value

was inhaled in the LPS group, the excessive inflammatory storm was scavenged ($p < 0.05$; Fig. 9A–E). In addition, the standard curves of rat inflammatory factors by ELISA kit are shown in Fig. 10.

Relationship between the protein levels of TLR4–NFκB–IL6/NLRP3 signaling pathway-related proteins and inflammatory factors

To verify the pivotal role of the TLR4–NFκB–IL6/NLRP3 signaling pathway in inhibiting the inflammatory response of H₂, the study performed Pearson correlation

analysis. The results showed that TLR4 was positively related to the level of degradation rate of IκBα (p -IκBα(s32)/IκBα) ($p < 0.05$; Fig. 11A), which was positively associated with the activated rate of NF-κB p65 (p -p65/NF-κB p65) ($p < 0.05$; Fig. 11B). A similar relationships were also found between p -p65/NF-κB p65 and the downstream factors including IL-6/CXCL1/CCL2 ($p < 0.05$, Fig. 11C–E). Another pathway also showed this positive correlation (p -p65/NF-κB p65 vs NLRP3/Casp1/IL-18/IL-1β) ($p < 0.05$, Fig. 11F–I).

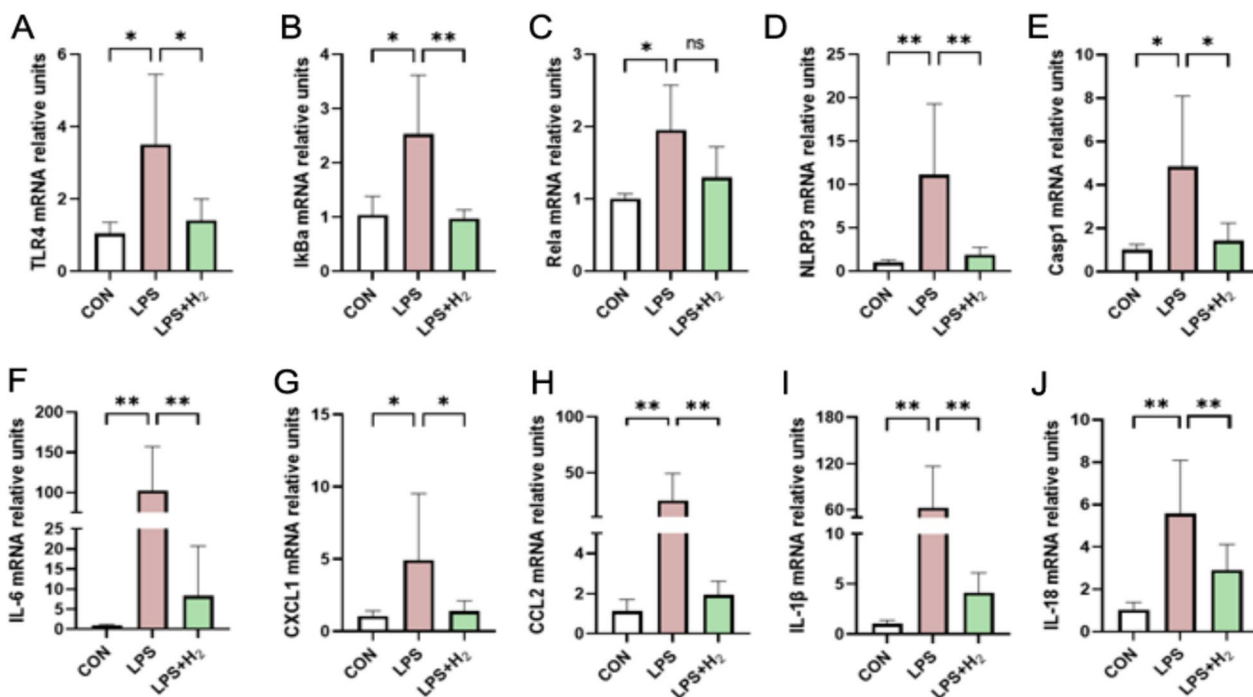


Fig. 7 mRNA levels of TLR4–NFκB–IL6/NLRP3 inflammatory signaling pathway in placenta. qRT-PCR analysis of relative mRNA levels of the genes in placenta. Bar graph shows mean ± SD of eight samples from each group, respectively. Data were displayed as mean ± SD. * $p < 0.05$, ** $p < 0.01$ vs LPS group

Discussion

Owing to serious complications and poor prognosis, BPD has been widely considered among LPS-induced adverse pregnancy outcomes [3]. BPD, manifested as lung injury, disrupts alveolarization and microvascular development [18]. Intra-amniotic administration of LPS at E16.5 to induce inflammatory cascades-CAM is similar to the major clinical characteristics observed in patients with BPD. LPS is derived from *E. coli* which is the most common pathogens leading to intrauterine infections in clinic, frequently applied to construct the intrauterine infection models. Intra-amniotic injection of LPS-induced CAM is one of the classic models that simulate pathological changes in BPD. The study chose to intra-amniotic injection of LPS in SD rats at E16.5 to cause intrauterine chorioamnionitis, because the lung tissue of fetal rat is in the transitional stage from tubular to vesicular stage at E16.5, which simulate and in line with the characteristics of clinical BPD (Premature infants, gestational weeks between 26 and 36 weeks, are in the vesicular stage of lung development and are prone to BPD in clinic). Intra-amniotic injection of LPS can accurately calculate the dosage of LPS according to experimental needs. However, the model still has drawbacks such as complex experimental operations, significant trauma, and susceptibility to infection.

CAM can produce excessive inflammatory factors in the fetus, which affect the maturation of the fetal lung, cause fetal lung structural remodeling, and affect the contractile function of pulmonary vessels, thus leading to the occurrence of BPD [19, 20]. Our results indicated that the LPS group exhibited a disorder of intrauterine development: intrauterine fetal death (IUID) rates were high in the LPS group. The surviving newborns also had a lower birth weight and placental weight than those in the CON group. Moreover, the results also revealed the poor outcomes of neonatal rats induced by LPS. The pups in the LPS group presented a growth-restricted state in the postnatal days, mainly in the lower body weight and lower survival ratio. Perturbed lung development (abnormal alveolarization and a severe inflammatory response) existed in LPS-induced newborns and was obviously lagging behind. Overall, LPS-induced lung injury was used as a model for BPD. Hydrogen gas is a novel therapeutic molecule, and its therapeutic potential in anti-apoptotic, anti-oxidative and anti-inflammatory effects has been recognized by many animal studies and clinical trials, especially in lung diseases [21, 22]. However, the inflammatory scavenging ability is a widely accepted mechanism of H₂ [7, 23]. In our research, H₂ was incorporated into the treatment of BPD as a therapeutic method. H₂ not

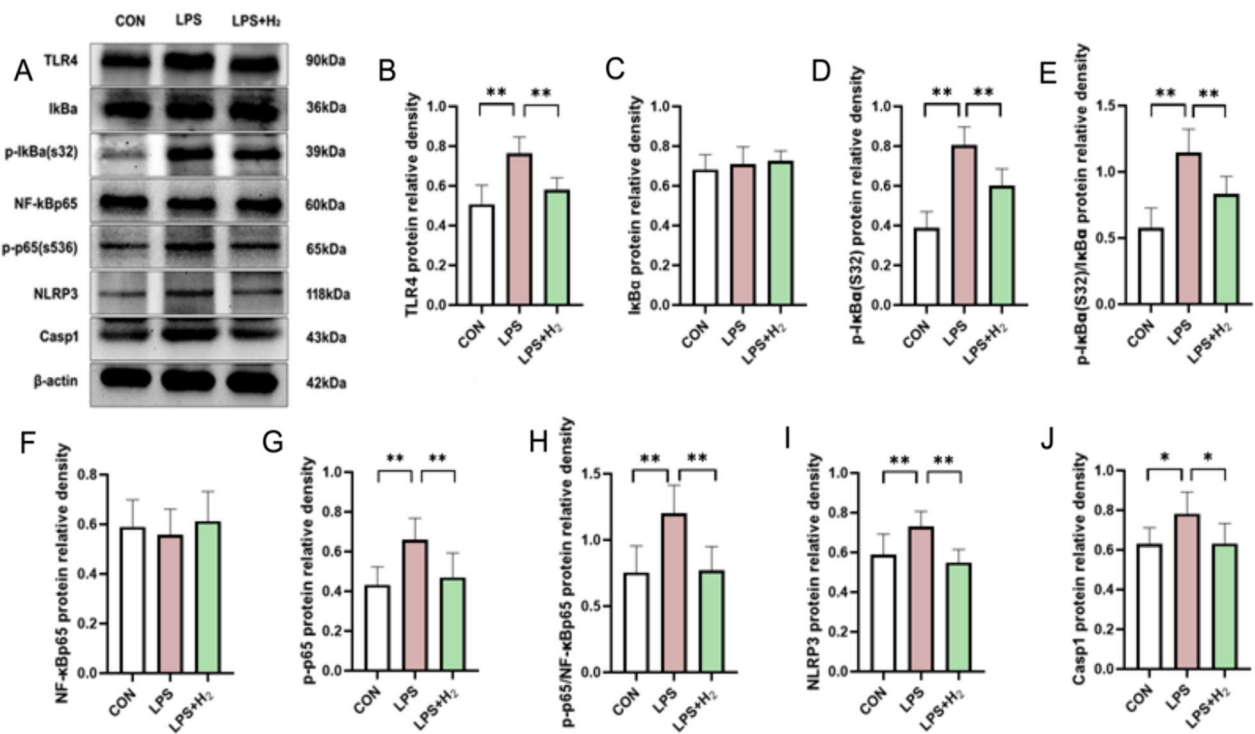


Fig. 8 Hydrogen downregulated the placental TLR4–NFκB-IL6/NLRP3 inflammatory signaling pathway to rescue from LPS-induced BPD. **A** A representative image of Western blots for TLR4, IkBa, Phospho-IkBa (Ser32) ((p-IkBa(s32)), NF-κB p65, NF-κB p65 (phospho S536)(p-p65), NLRP3 and Casp1 in placenta from each group. β-actin was used to verify equivalent loading. Graphic representation of relative density of TLR4 (**B**), IkBa (**C**), p-IkBa(s32) (**D**), NF-κB p65 (**F**), p-p65(s536) (**G**), NLRP3 (**I**) and Casp1 (**J**) normalized to β-actin. Graphic representation of relative abundance of p-IkBa(s32)/IkBa (**E**) and p-p65/NF-κB p65 (**H**). Data were presented as mean ± SD of 8 samples from each group. **p* < 0.05, ***p* < 0.01 vs LPS group

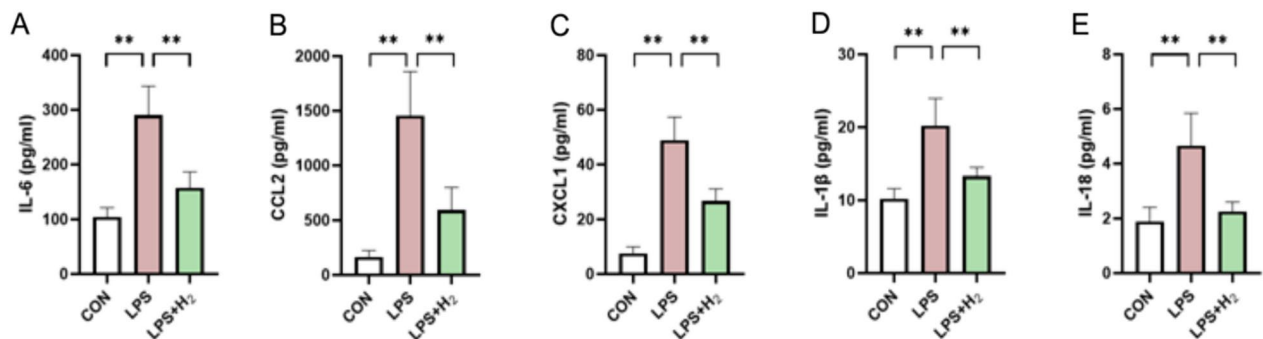


Fig. 9 H₂ relieved the excessive inflammatory cytokines and chemokines in LPS-induced BPD, as detected by ELISA. **A–E** Graphic representation of protein levels of IL-6 (**A**), CCL2 (**B**), CXCL1 (**C**), IL-1β (**D**) and IL-18 (**E**) in the placenta. Data were presented as mean ± SD of 8 samples from each group. **p* < 0.05, ***p* < 0.01 vs LPS group

only attenuated the abnormal intrauterine development by reducing the IUFD and ameliorating the loss to fetus induced by LPS, but also improved the poor outcomes of neonatal rats by normalizing the LPS-induced perturbed lung development. Our findings indicated that H₂ inhalation was indeed a promising candidate for BPD treatment, and the mechanism was deeply elucidated in this research.

Recent studies have revealed that imbalanced proinflammatory and anti-inflammatory cytokines in the placenta play a major role in the pathophysiology of BPD, characterized by excessive inflammatory response syndrome, which acts as an exposure risk factor that contributes to the development of BPD [9, 24]. Placental compositions, consisting of cytokines, chemokines and natural antioxidants, have direct consequences

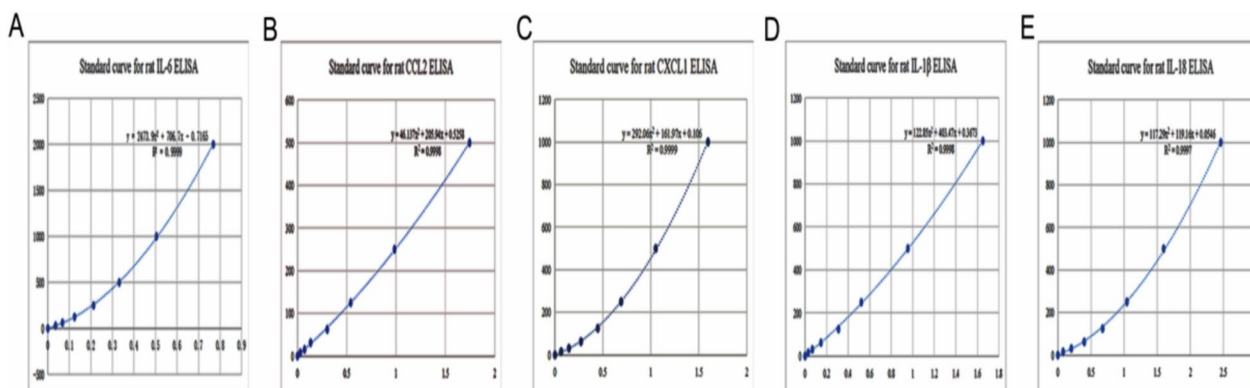


Fig. 10 The standard curve of rat inflammatory factors by ELISA kit. A-E Represented the standard curves for IL-6 (A), CCL2 (B), CXCL1 (C), IL-1 β (D) and IL-18 (E), respectively

on the inflammatory response via anti-inflammatory, anti-bacterial and anti-viral properties [25, 26]. It is conceivable that disturbances in placental biochemical composition and in the placental signaling pathway contribute to the pathophysiology of BPD. Our results showed an excessive inflammatory response in the LPS-induced placenta in rats, and inflammatory cells were scattered in the umbilical artery. Combined with the correlation analysis results (placental weight versus birth weight), there is no doubt that placental dysfunction plays a critical role in the development of BPD.

Previous studies have confirmed that H_2 can exert anti-inflammatory effects in a variety of cells through multiple signaling pathways. For instance, H_2 can reduce the expression of intercellular adhesion molecules and chemokines to reduce the infiltration of neutrophils and macrophages [27, 28]. In a study of rat burns, H_2 also alleviated the airway inflammatory response by reducing the activation of the crucial NF- κ B-mediated inflammatory signaling pathway, subsequently reducing IL-1 β and IL-6 levels [29]. Currently, researchers have also found the perspectives of H_2 for coronavirus disease-2019 (COVID-19) caused by severe acute respiratory syndrome coronavirus 2 (SARS-CoV-2). COVID-19 manifests as acute inflammatory lung injury caused by a cytokine storm, H_2 inhalation plays a notable role in annihilating inflammatory cytokines to inhibit cytokine storms. Due to the remarkable anti-inflammatory effect of H_2 , it has been recommended in acute or chronic pulmonary disease to eventually confront the COVID-19 pandemic [30–33]. Our results were consistent with a previous study: H_2 inhalation moderated the excessive inflammatory response of LPS-treated placentas in rats, including reducing the degree of infiltration and significantly narrowing the range of infiltration. The fetal inflammatory reaction was equally mitigated upon

administration of H_2 , as reflected by the umbilical artery histology.

BPD has been generally acknowledged as a complicated pathological process involving complex and redundant molecules and signaling pathways. Inflammation response is an extremely important link in the development of BPD. The placenta is a natural immune barrier for the fetus to resist pathogenic microbial infections. It can recognize pathogenic microorganisms, generate immune responses at the maternal–fetal interface, and play a role in inflammatory regulation. Placental trophoblast cells, as the first layer of immune defense, mainly express TLR4. During intrauterine infection, the expression of TLR4 mRNA in placental tissue is significantly increased and consistent with the degree of CAM, activating downstream factors IL-6, IFN- γ , IL-4 to an inflammatory cascade, ultimately leading to fetal inflammatory response syndrome. Research has found that inhibiting the expression of TLR4 in the placenta can significantly reduce the release of downstream factors, reduce inflammatory reactions, and significantly improve adverse outcomes in newborns, which has been found in hepatitis B virus infection, *E. coli* intrauterine infection and other studies. The anti-inflammatory signaling pathway mediated by TLR4 has also attracted increasing attention in diseases caused by intrauterine infections. As an important member of toll-like receptors family, TLR4, mainly stimulated by LPS, is a major inflammatory messenger that is widely involved in inflammation response. The inflammatory cascade triggered by TLR4 drives the severity of intra-amniotic inflammation in pregnancy and impacts lung development [34, 35]. NF- κ B is a downstream signaling linked by TLR4. LPS could directly induce TLR4 and activation of NF- κ B signaling, which in turn led to production of inflammatory factors [36, 37]. Given the

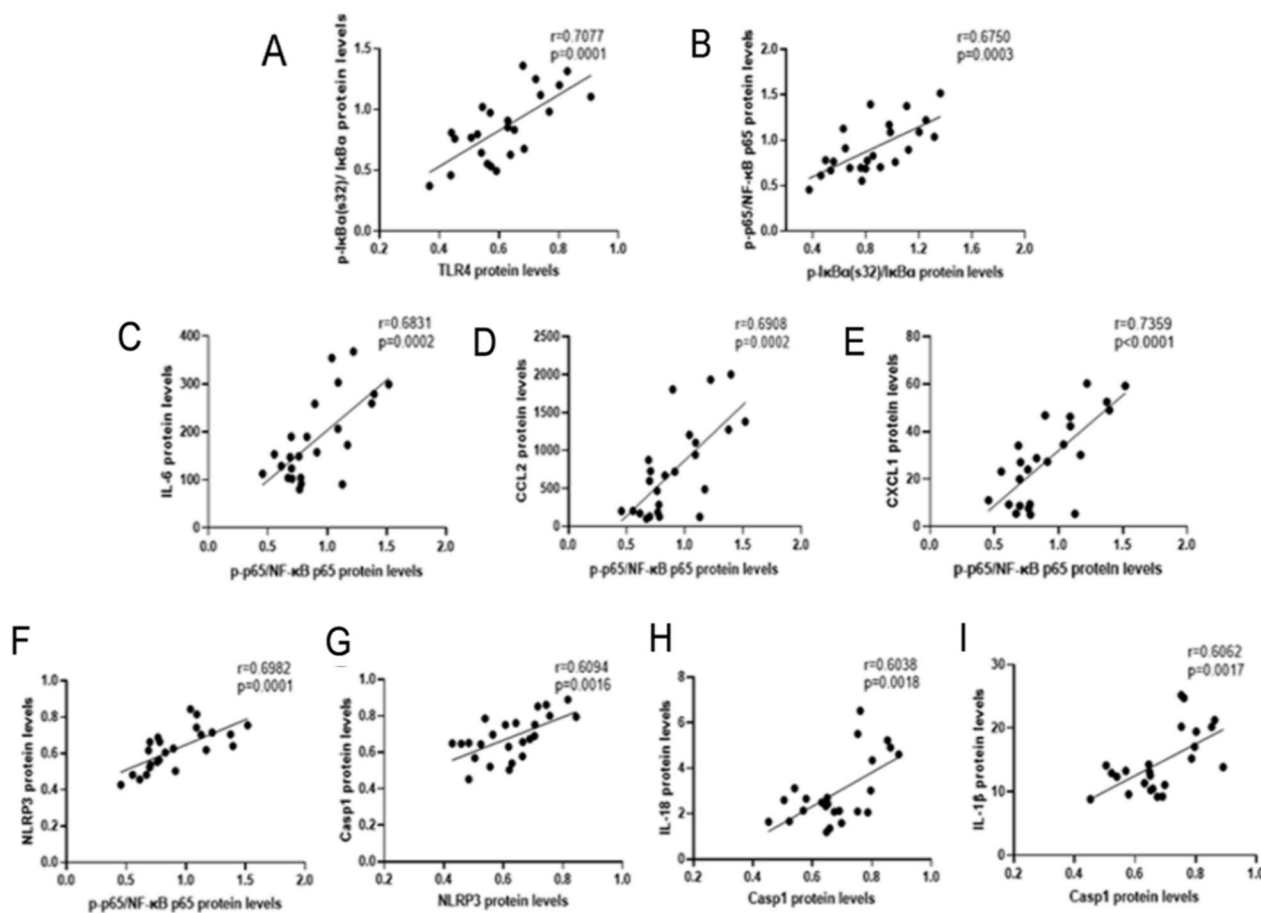


Fig. 11 The relationships between TLR4–NFκB–IL6/NLRP3 and the protein levels of inflammatory cytokines/chemokines in placentas. **A** Relationship between TNF-α and placental p-IκBα(s32)/IκBα levels in all groups; **B** p-IκBα(s32)/IκBα vs p-p65/NF-κB p65; **C** p-p65/NF-κB p65 vs IL-6; **D** p-p65/NF-κB p65 vs CCL2; **E** p-p65/NF-κB p65 vs CXCL1; **F** p-p65/NF-κB p65 vs NLRP3; **G** NLRP3 vs Casp1; **H–I** Casp1 vs IL-18 and Casp1 vs IL-1β; $n = 24$, $r =$ Pearson's correlation coefficient

role of TLR4/NF-κB signaling pathway in inflammation, we investigated the beneficial effect of inhaled H₂ on LPS-induced BPD, and we raised the question: does hydrogen inhibit inflammation by downregulating the expression of the hub protein TLR4 and subsequently reducing the activity of the NF-κB-mediated inflammatory signaling pathway? TLR4 is stably expressed in both the first and third trimester placental trophoblast cells, recognizing LPS to initiate the intracellular cascade. Activation of TLR4 by LPS can promote phosphorylation of IκBα. In the physiological state, IκBα, as the strongest negative feedback factor in NF-κB activation, bound with NF-κB dimers (p50 with p65) in the cytoplasm to inhibit NF-κB activation. The activation of TLR4 can strengthen the phosphorylation of IκBα (p-IκBα) to get rid of the inactivation state of the NF-κB dimers. Subsequently, the exposure of the nuclear localization signal region (NLS) of NF-κB and induced the phosphorylation of NF-κB p65 (p-p65) pass into the nucleus, which could bind to KB

sites on the promoters of regulatory genes to initiate gene transcription to mediate the inflammatory response. The p-p65 can enhance the mRNA transcription of IL-6, IL-1β and IL-18 to promote the production and release of proinflammatory factors. At the same time, the increased expression of IL-6 has ability to amplify the initial inflammatory signal, result in inflammatory cascade and aggravating cell damage. It can also regulate the expression of chemokines such as CXCL1 and CCL2, thus recruiting massive mononuclear macrophages and neutrophils, and triggering inflammatory infiltration and damage. Recent studies have found that TLR4 can also mediate the NLRP3-mediated inflammatory signaling pathway through the activation of NF-κB. The biological effects of the NLRP3 inflammasome in inflammatory diseases have received extensive attention. The activated NF-κB can stimulate the mRNA transcription of the NLRP3 inflammasome to a great extent in the nucleus, which can aggregate in response to cellular perturbations

to drive inflammatory states. Activation of NLRP3 transforms the immature pro-caspase1 into the active effector protein caspase1 (Casp1). Casp1 can not only directly punch in the cell membrane to cause cell death, and release intracellular inflammatory factors after its lysis, but also promote the maturation and release of inflammatory cytokines IL-1 β and IL-18, resulting in inflammatory cell death.

As we conceived, the toll-like receptor signaling pathway and inflammatory response biological process in placenta were strikingly located in RNA-seq results. Significantly differentially expressed genes between the LPS and LPS + H₂ groups also revealed possible relevant downstream factors. Among them, the downstream signaling factors surrounding the NF- κ B as the hub were prominently highlighted. Therefore, we identified and evaluated alterations in the TLR4/NF- κ B-mediated signaling pathways in the placentas of the CON, LPS and LPS+H₂ groups and the relevant intensity

between them. The results demonstrated that H₂ inhalation largely ameliorated the increased mRNA and protein levels of TLR4 induced by LPS in the placenta ($p < 0.05$). The same phenomena were also reflected in the degree of I κ B α degradation (p-I κ B α (s32)/I κ B α) and NF- κ B p65 activation (p-p65/NF- κ B p65) [38], the downstream activated factors NLRP3 and caspase1, concomitantly. Consistently, excessive inflammatory cytokines and chemokines in response to LPS were also scavenged by H₂ inhalation, including IL-6, IL-18, IL-1 β , CCL2 and CXCL1. Proteins are messengers of biological function, and identifying the relevant intensity of those proteins was conducive to reflecting the pivotal role of the TLR4/NF- κ B-mediated signaling pathway in regulating the downstream inflammatory cytokines/chemokines [39]. The data confirmed that positive associations of TLR4 versus NF- κ B and NF- κ B versus the downstream signaling factors (NLRP3, Casp1, CXCL1, CCL2, IL-6) were consistent with the

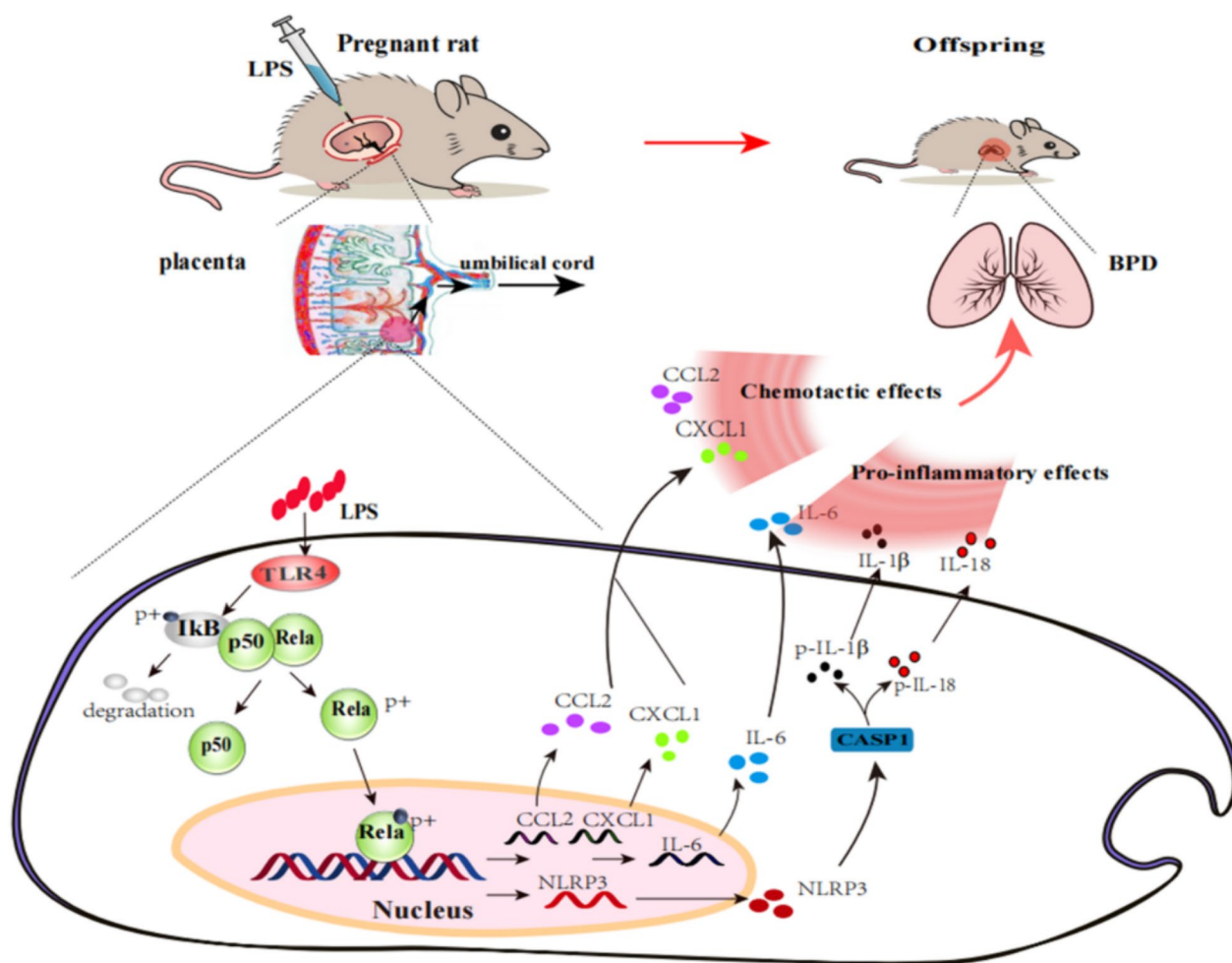


Fig. 12 Hydrogen inhalation reduces the occurrence of LPS-induced BPD

role of TLR4 in previous studies. The impacts on the placenta were consistent with the outcomes of neonatal lung of different groups in this study, subsequently. Administration of hydrogen reduced the LPS-induced BPD by significantly lessening placental inflammatory factors (IL-6, IL-18, IL-1 β , CCL2, CXCL1, NLRP3 and Casp1) to fetal circulation, then further proceeded to alleviate the FIRS and reduced the infiltration of proinflammatory cells in fetal lung tissue, resulting in the increased amount of alveoli and the decreased area of pulmonary septum to ultimately normalize the disorder of neonatal BPD induced by LPS.

Combined with relevant relationships, we can hypothesize that TLR4 contributes to the therapeutic effect of hydrogen inhalation on LPS-induced BPD by regulating the NF- κ B-mediated inflammatory signaling pathway, resulting in the scavenging of excessive inflammatory cytokines and chemokines. The mechanism is shown in Fig. 12.

Conclusion

In conclusion, our study demonstrated that H₂ inhalation significantly rescued LPS-induced BPD, and the alleviation of LPS-induced BPD by H₂ inhalation was mainly dependent on the inhibition of the TLR4–NF κ B–IL6/NLRP3-mediated signaling pathway, eventually resulting in scavenging inflammatory cytokines/chemokines. Consequently, hydrogen gas inhalation under CAM in pregnancy may become an effective treatment to improve their poor outcomes.

Abbreviations

BPD	Bronchopulmonary dysplasia
H ₂	Hydrogen
LPS	Lipopolysaccharide
CAM	Chorioamnionitis
FIRS	Fetal inflammatory response syndrome
IL	Interleukin
CCL2	C–C Motif chemokine ligand 2
CXCL1	C–X–C Motif chemokine ligand 1
TLR4	Toll-like receptor 4
NF- κ B	Nuclear factor kappa-B
NLRP3	NLR family pyrin domain containing 3
Casp1	Caspase 1
CCL2	C–C motif chemokine ligand 2
CXCL1	C–X–C motif chemokine ligand 1
KEGG	Kyoto Encyclopedia of Genes and Genomes
TUNEL	TdT-mediated dUTP Nick-end labeling
HE	Hematoxylin–eosin
MLI	The mean linear intercept
RAC	Radial alveolar count
GO	Gene Ontology
IUFD	The intrauterine fetal death
BW	Birth weight
P14	Postnatal day 14

Acknowledgements

We acknowledge the participants and the Central Laboratory of Taian City Central Hospital for technical support.

Author contributions

YFZ drafted the manuscript. LLZ and ZXC analyzed data. YW and GY contributed to concept and designed the study. YFZ, XHR, YXC and YT performed the research, WJL and XLS provided the technical support. YZW, YW and GY revised and made suggestions for final revisions. All authors read and approved the final manuscript.

Funding

This study was supported by Shandong Provincial Medical Employee Science and Technology Innovation Program Project, China (SDYWZGKCJHLH2023097 to Yafang Zhang), Taian City Science and Technology Program, China (2021NS327 to Yafang Zhang), and Shandong Provincial Natural Science Foundation, China (ZR2021MH025 to Qingbin Ni).

Availability of data and materials

The raw RNA sequencing data supporting the conclusions of this article are available in the NCBI Sequence Read Archive (SRA) database with accession number PRJNA901070. The datasets used and analyzed during the current study are available from the corresponding author on reasonable request.

Declarations

Ethics approval and consent to participate

All experimental procedures were approved by the Medical Ethics Committee of the affiliated Taian City Central Hospital of Qingdao University, China (permit numbers: 2022-07-10).

Consent for publication

Not applicable.

Competing interests

The authors declare no competing interests.

Author details

¹Department of Neonatology and NICU, The Affiliated Taian City Central Hospital of Qingdao University, Taian, Shandong, China. ²Medical Imaging Center, The Affiliated Taian City Central Hospital of Qingdao University, Taian, Shandong, China. ³Central Laboratory, The Affiliated Taian City Central Hospital of Qingdao University, Taian, Shandong, China. ⁴Department of Ultrasound, Taian Traditional Chinese Medicine Hospital, Taian, Shandong, China. ⁵Research Center for Translational Medicine, Tongji University Affiliated East Hospital, Shanghai, China.

Received: 4 March 2024 Accepted: 28 April 2024

Published online: 14 May 2024

References

- Schmidt AR, Ramamoorthy C. Bronchopulmonary dysplasia. *Paediatr Anaesth.* 2022;32:174–80.
- Gilfillan M, Bhandari A, Bhandari V. Diagnosis and management of bronchopulmonary dysplasia. *BMJ.* 2021;375: n1974.
- McGrath-Morrow SA, Collaco JM. Bronchopulmonary dysplasia: what are its links to COPD? *Ther Adv Respir Dis.* 2019;13:1753466619892492.
- Papagianis PC, Pillow JJ, Moss TJ. Bronchopulmonary dysplasia: Pathophysiology and potential anti-inflammatory therapies. *Paediatr Respir Rev.* 2019;30:34–41.
- Villamor-Martinez E, Alvarez-Fuente M, Ghazi AMT, Degraeuwe P, Zimmermann LJ, Kramer BW, Villamor E. Association of chorioamnionitis with bronchopulmonary dysplasia among preterm infants: a systematic review, meta-analysis, and metaregression. *JAMA Netw Open.* 2019;2: e1914611.
- Mir IN, Chalak LF, Brown LS, Johnson-Welch S, Heyne R, Rosenfeld CR, Kapadia VS. Impact of multiple placental pathologies on neonatal death, bronchopulmonary dysplasia, and neurodevelopmental impairment in preterm infants. *Pediatr Res.* 2020;87:885–91.
- Budal EB, Ebbing C, Kessler J, Bains S, Haugen OH, Aukland SM, Eide GE, Halvorsen T, Bentsen MHL, Collett K. Placental histology predicted

- adverse outcomes in extremely premature neonates in Norway-population-based study. *Acta Paediatr.* 2022;111:546–53.
8. McCartney SA, Kapur R, Liggitt HD, Baldessari A, Coleman M, Orvis A, Ogle J, Katz R, Rajagopal L, Adams Waldorf KM. Amniotic fluid interleukin 6 and interleukin 8 are superior predictors of fetal lung injury compared with maternal or fetal plasma cytokines or placental histopathology in a nonhuman primate model. *Am J Obstet Gynecol.* 2021;225(89):e81–89 e16.
 9. Rallis D, Lithoxopoulou M, Pervana S, Karagianni P, Hatzioannidis I, Soubasi V, Tsakalidis C. Clinical chorioamnionitis and histologic placental inflammation: association with early-neonatal sepsis. *J Matern Fetal Neonatal Med.* 2021;35:1–7.
 10. Goncalves LF, Cornejo P, Towbin R. Neuroimaging findings associated with the fetal inflammatory response syndrome. *Semin Fetal Neonatal Med.* 2020;25: 101143.
 11. Nie C, Ding X, Rong A, Zheng M, Li Z, Pan S, Yang W. Hydrogen gas inhalation alleviates myocardial ischemia-reperfusion injury by the inhibition of oxidative stress and NLRP3-mediated pyroptosis in rats. *Life Sci.* 2021;272: 119248.
 12. Tian Y, Zhang Y, Wang Y, Chen Y, Fan W, Zhou J, Qiao J, Wei Y. Hydrogen, a novel therapeutic molecule, regulates oxidative stress, inflammation, and apoptosis. *Front Physiol.* 2021;12:2281.
 13. Yang M, Dong Y, He Q, Zhu P, Zhuang Q, Shen J, Zhang X, Zhao M. Hydrogen: a novel option in human disease treatment. *Oxid Med Cell Longev.* 2020;2020:8384742.
 14. Wu Y, Yuan M, Song J, Chen X, Yang H. Hydrogen gas from inflammation treatment to cancer therapy. *ACS Nano.* 2019;13:8505–11.
 15. Zhuang X, Yu Y, Jiang Y, Zhao S, Wang Y, Su L, Xie K, Yu Y, Lu Y, Lv G. Molecular hydrogen attenuates sepsis-induced neuroinflammation through regulation of microglia polarization through an mTOR-autophagy-dependent pathway. *Int Immunopharmacol.* 2020;81: 106287.
 16. Cole AR, Raza A, Ahmed H, Polizzotti BD, Padera RF, Andrews N, Kheir JN. Safety of inhaled hydrogen gas in healthy mice. *Med Gas Res.* 2019;9:133–8.
 17. Cole AR, Sperotto F, DiNardo JA, Carlisle S, Rivkin MJ, Sleeper LA, Kheir JN. Safety of prolonged inhalation of hydrogen gas in air in healthy adults. *Crit Care Explor.* 2021;3: e543.
 18. Thebaud B, Goss KN, Laughon M, Whitsett JA, Abman SH, Steinhorn RH, Aschner JL, Davis PG, McGrath-Morrow SA, Soll RF, Jobe AH. Bronchopulmonary dysplasia. *Nat Rev Dis Primers.* 2019;5:78.
 19. Hillman NH, Kemp MW, Fee E, Rittenschober-Bohm J, Roysse E, Abugisisa L, Salomone F, Musk GC, Jobe AH. Budesonide with surfactant decreases systemic responses in mechanically ventilated preterm lambs exposed to fetal intra-amniotic lipopolysaccharide. *Pediatr Res.* 2021;90:328–34.
 20. Papagianis PC, Ahmadi-Noorbakhsh S, Lim R, Wallace E, Polglase G, Pillow JJ, Moss TJ. The effect of human amnion epithelial cells on lung development and inflammation in preterm lambs exposed to antenatal inflammation. *PLoS ONE.* 2021;16: e0253456.
 21. Ohta S. Molecular hydrogen as a preventive and therapeutic medical gas: initiation, development and potential of hydrogen medicine. *Pharmacol Ther.* 2014;144:1–11.
 22. Qi B, Yu Y, Wang Y, Wang Y, Xie K. Perspective of molecular hydrogen in the treatment of sepsis. *Curr Pharm Des.* 2021;27:667–78.
 23. Alwazeer D, Liu FF, Wu XY, LeBaron TW. Combating oxidative stress and inflammation in COVID-19 by molecular hydrogen therapy: mechanisms and perspectives. *Oxid Med Cell Longev.* 2021;2021:5513868.
 24. Matsuura H, Matsumoto H, Okuzaki D, Shimizu K, Ogura H, Ebihara T, Matsubara T, Hirano SI, Shimazu T. Hydrogen gas therapy attenuates inflammatory pathway signaling in septic mice. *J Surg Res.* 2021;263:63–70.
 25. Cookson MW, Ryan SL, Seedorf GJ, Dodson RB, Abman SH, Mandell EW. Antenatal vitamin D preserves placental vascular and fetal growth in experimental chorioamnionitis due to intra-amniotic endotoxin exposure. *Am J Perinatol.* 2018;35:1260–70.
 26. Kim CJ, Romero R, Chaemsaitong P, Chaiyasit N, Yoon BH, Kim YM. Acute chorioamnionitis and funisitis: definition, pathologic features, and clinical significance. *Am J Obstet Gynecol.* 2015;213:S29–52.
 27. Zhao S, Mei K, Qian L, Yang Y, Liu W, Huang Y, Zhang C, Sun X, Liu C, Li B, et al. Therapeutic effects of hydrogen-rich solution on aplastic anemia in vivo. *Cell Physiol Biochem.* 2013;32:549–60.
 28. Chen M, Zhang J, Chen Y, Qiu Y, Luo Z, Zhao S, Du L, Tian D. Hydrogen protects lung from hypoxia/re-oxygenation injury by reducing hydroxyl radical production and inhibiting inflammatory responses. *Sci Rep.* 2018;8:8004.
 29. Wang X, Yu P, Yong Y, Liu X, Jiang J, Liu D, Xue G. Hydrogen-rich saline resuscitation alleviates inflammation induced by severe burn with delayed resuscitation. *Burns.* 2015;41:379–85.
 30. Wang ST, Bao C, He Y, Tian X, Yang Y, Zhang T, Xu KF. Hydrogen gas (XEN) inhalation ameliorates airway inflammation in asthma and COPD patients. *QJM.* 2020;113:870–5.
 31. Fara A, Mitrev Z, Rosalia RA, Assas BM. Cytokine storm and COVID-19: a chronicle of pro-inflammatory cytokines. *Open Biol.* 2020;10: 200160.
 32. Ye Q, Wang B, Mao J. The pathogenesis and treatment of the 'Cytokine Storm' in COVID-19. *J Infect.* 2020;80:607–13.
 33. Guan WJ, Chen RC, Zhong NS. Strategies for the prevention and management of coronavirus disease 2019. *Eur Respir J.* 2020;55:2000597.
 34. Lai JL, Liu YH, Liu C, Qi MP, Liu RN, Zhu XF, Zhou QG, Chen YY, Guo AZ, Hu CM. Indirubin inhibits LPS-induced inflammation via TLR4 abrogation mediated by the NF- κ B and MAPK signaling pathways. *Inflammation.* 2017;40:1–12.
 35. Rocha DM, Caldas AP, Oliveira LL, Bressan J, Hermsdorff HH. Saturated fatty acids trigger TLR4-mediated inflammatory response. *Atherosclerosis.* 2016;244:211–5.
 36. Jiang B, Wang D, Hu Y, Li W, Liu F, Zhu X, Li X, Zhang H, Bai H, Yang Q, et al. Serum amyloid A1 exacerbates hepatic steatosis via TLR4-mediated NF- κ B signaling pathway. *Mol Metab.* 2022;59: 101462.
 37. Ahmed M, Casanova NG, Zaghoul N, Gupta A, Rodriguez M, Robbins IR, Kempf CL, Sun X, Song JH, Hernon VR, et al. The eNAMPT/TLR4 inflammatory cascade drives the severity of intra-amniotic inflammation in pregnancy and predicts infant outcomes. *Front Physiol.* 2023;14:1129413.
 38. Shen J, Cheng J, Zhu S, Zhao J, Ye Q, Xu Y, Dong H, Zheng X. Regulating effect of baicalin on IKK/ κ B/NF- κ B signaling pathway and apoptosis-related proteins in rats with ulcerative colitis. *Int Immunopharmacol.* 2019;73:193–200.
 39. Zusso M, Lunardi V, Franceschini D, Pagetta A, Lo R, Stifani S, Frigo AC, Giusti P, Moro S. Ciprofloxacin and levofloxacin attenuate microglia inflammatory response via TLR4/NF- κ B pathway. *J Neuroinflammation.* 2019;16:148.

Publisher's Note

Springer Nature remains neutral with regard to jurisdictional claims in published maps and institutional affiliations.